Molecular-dynamics investigations of shock-induced detonations in inhomogeneous energetic crystals

P. Maffre and M. Peyrard
Physique Non-Linéaire: Ondes et Structures Cohérentes, Faculté des Sciences, 6 blvd. Gabriel, 21000 Dijon, France
(Received 24 July 1991)

The propagation of shock-induced detonations in an inhomogeneous sample is studied at the microscopic level by molecular dynamics. The model consists of a two-dimensional lattice of diatomic molecules connected by Morse potentials. A predissociative intramolecular potential is used. Simulations in a perfect crystal exhibit two detonation regimes: a fast regime, in which the atomic motions are very coherent, and a slow regime, which is the regime observed experimentally. The propagation of the detonation wave across grain boundaries, domains with a different orientation, vacancies, and a region where the chemical reaction started earlier due to a hot spot, is investigated. The slow-detonation regime is found to be very robust, showing that the structure observed at the microscopic level could persist in a real polycrystalline sample. The fast-denonation regime is highly sensitive to perturbations and tends to evolve into fingerlike structures. Its possible relevance in some systems is discussed.

I. INTRODUCTION

Although the detonation process is now well known on a macroscopic scale, its understanding at the microscopic level is still very poor.[1] The macroscopic approaches can be rather successful for dilute gases, but they fail to provide a proper description of shock-induced detonations in condensed phases, and particularly in solids. Among the unexplained features are the correlations found experimentally between detonation properties of energetic materials and their crystal structures[2] or the large anisotropies in detonation speeds and directional sensitivity of monocrystals to shocks.[3] Moreover, recent experiments in fluids[4] suggest that the width of a shock front in a condensed phase is of the order of a few atomic distances, so that the assumption of thermal equilibrium in the wake of the shock, which is at the basis of the macroscopic thermodynamic approach, is questionable. One of the difficulties to propose a microscopic theory of detonations is the lack of experimental information at the molecular level due to the extremely high space and time resolution that would be required. Consequently, numerical simulation is a useful tool to improve our microscopic understanding of detonations because its resolution is sufficient to determine the motion of a single atom.

There are, however, two kinds of limitation to the molecular-dynamics investigations of energetic materials. The first one is the speed of the available computers that confines the simulations to simple models or very small samples. Considering the current progress in computer techniques, this type of limitation is fading. The second limitation, which is related to the design of the simulation model, is more fundamental because the detonation process is a very complex one involving not only the dynamics of the atoms or molecules, but also chemical reactions and very different time scales. These various problems have been addressed one after the other since the calculations performed by Karo, Hardy, and Walker[5] and Tsai and Trevino.[6,7] The usual approach represents the chemical reactions by a so-called "predissociative potential" to provide energy release during reaction. Two different approaches have been used to improve the description of the detonation chemistry. The first one incorporates a bond-breaking and bond-forming mechanism by using three-body interactions[8,9] or by introducing chemical effects by a model, which could, in principle, include quantum effects although it is not yet the case, embedded in a molecular-dynamics calculation.[10]

In this work we address another problem for the microscopic simulation of detonations, the role of crystal inhomogeneities or defects on the propagation of the detonation wave. It is an important question because real energetic materials are seldom good monocrystals and inhomogeneities are known to have a large influence at the macroscopic scale. At the microscopic level, defects can be viewed as having two opposite roles; they may break the coherent propagation of the detonation wave that is observed in the molecular-dynamics simulations of perfect crystals,[11,12] or they may create hot spots which help molecular dissociations and sustain the detonation. These two aspects are analyzed in the present work. Section II presents and discusses the model that we have developed for this investigation. The properties of this model in the case of a homogeneous sample are presented in Sec. III as a reference case for Sec. IV which examines the role of various inhomogeneities.

II. THE MOLECULAR-DYNAMICS MODEL

It is tempting to include in one single study all the state-of-the-art techniques for modeling an energetic crystal, for instance, three-body potentials[8] or the constrained molecular-dynamics method that we have developed previously to simulate the chemistry.[10] However, in the presence of inhomogeneities, there is another important constraint due to the minimum size of the sample required to get meaningful results. This size must be significantly larger than the size of the defects that we

wish to study. Moreover, in order to get rid of possible artefacts due to the initiation in an inhomogeneous material, we initiate the detonation in a homogeneous sample and wait until it has reached a steady state before introducing an inhomogeneous part in the model so that we must follow the detonation wave for a longer period than in a homogeneous sample. Consequently, we have chosen to work with a rather simple model using the predissociative potential in order to allow sufficiently fast simulations. It is derived from the model that we used in a previous investigation.[12] In its original form, this model was designed with emphasis on the investigation of the solid phase in order to determine the structure of the detonation wave in the immediate vicinity of the front. In this region, although it is severely perturbed, the crystal structure is not completely destroyed. In particular, the neighbors of a given atom do not vary significantly. Thus, provided that the number of neighbors included in the force calculation is sufficiently large, it is not necessary to check dynamically for the neighbors. This is an important computation time saving and it allows the design of an efficient algorithm on a vector computer. This approach is no longer acceptable if the model is designed to study the dynamics of crystal defects. For instance, when a dislocation moves, bond rearrangements take place. Consequently, although the basic ideas of the original model are conserved, the new version has been significantly modified and the program has been completely rewritten.

A. The model crystal

The model crystal is shown in Fig. 1. It consists of a two-dimensional array of two-component molecules. The components are henceforth denoted as "atoms" N and C. However, in a real crystal like the nitromethane crystal that we use as a reference case to determine the potential parameters, they could represent more complex groups like NO_2 and CH_3. The intramolecular potential which connects the N and C atoms, which comprise the N-C molecule, is the predissociative exothermic potential shown in Fig. 2. Such a potential, which was found

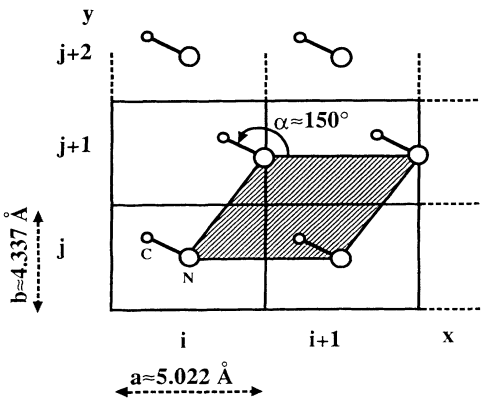

FIG. 1. Schematic picture of the model crystal. The hatched area is the oblique primitive unit cell. For computational convenience a rectangular grid is used to label the molecules (indices i and j).

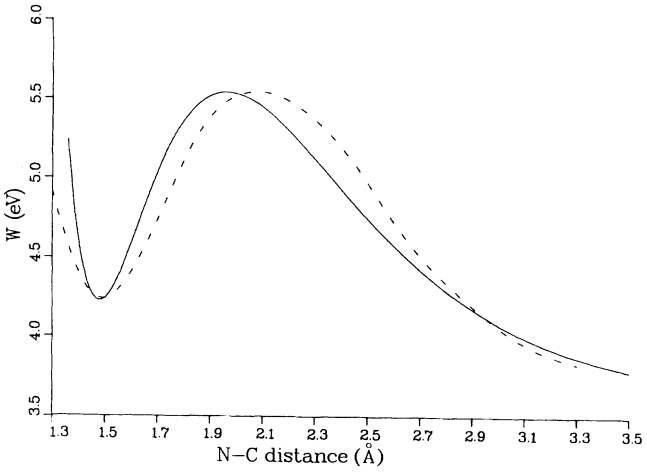

FIG. 2. The predissociative intramolecular potential. Dotted line: potential of the predissociative excited state of nitromethane (from Ref. 13). Solid line: intramolecular potential, the difference between two Morse potentials before the rescaling of the energies performed to correct the sound speed.

among the first excited states of nitromethane, provides an approximate description of the chemistry of the detonation in a form compatible with molecular dynamics. When the two atoms are separated by their equilibrium distance r_0, the molecule is stable. If the molecule is subjected to a strong perturbation, it can dissociate through an endothermic process which brings the bond to its dissociation length r_D. Then, in a second step, some potential energy is released while the bond length extends further. This exothermic step models the reactions which follow the dissociation in a real detonation. The repulsion of the N and C atoms during this step increases their kinetic energy and sustains the shock. For computational convenience, the predissociative intramolecular potential is written as the difference between two Morse potentials as

$$\begin{aligned} W(r_{1,2}) &= V_a(r_{1,2}) - V_b(r_{1,2}) \\ &= E_a\{\exp[-S_a(r_{1,2}-r_0)]-1\}^2 \\ &\quad -E_a - E_b\{\exp[-S_b(r_{1,2}-r_0)]-1\}^2 + E_b \ , \end{aligned} \tag{1}$$

where $r_{1,2}$ is the length of the intramolecular N-C bond, E_a and E_b are the dissociation energies of the two Morse potentials, and S_a and S_b are their anharmonic coefficients. The shape shown in Fig. 2 is obtained if $E_a < E_b$ and $S_a > S_b$. The difference $E_b - E_a$ measures the energy released when the N-C molecule is dissociated.

The N-C molecules are bonded to one another by intramolecular Morse potentials

$$V(r) = E\{\exp[-S(r-r_e)]-1\}^2 - E \ , \tag{2}$$

where r is the bond length. Three different potentials, i.e., three sets of constants E, S, and r_e, are used for the three types of intermolecular bonds in the model crystal, N-N, C-C, and N-C. The Hamiltonian of the crystal is therefore

$$H=\sum_{i,j}\left[\tfrac{1}{2}m_1\{[\dot{x}_1(i,j)]^2+[\dot{y}_1(i,j)]^2\}+\tfrac{1}{2}m_2\{[\dot{x}_2(i,j)]^2+[\dot{y}_2(i,j)]^2\}\right.$$
$$\left.+W(r_{1,2}(i,j))+\tfrac{1}{2}\sum_{s,k,l,s'(k,l\neq i,j)}V_{s,s'}(r_{s,s'}(i,j,k,l))\right], \quad (3)$$

where the indices $s=1,2$ and $s'=1,2$ designate, respectively, the N and C atoms at grid indices (i,j) and (k,l) separated by $r_{s,s'}(i,j,k,l)$.

The structure of the two-dimensional model crystal is imposed by the bond scheme. It is the structure which minimizes the Hamiltonian (3). We determine it by a numerical relaxation of an initial configuration with a pseudodynamical method.[14] A test sample containing 20×20 molecules is relaxed until a steady configuration at zero temperature is achieved. The final structure is the oblique structure shown in Fig. 1 which is henceforth called the reference structure. For computational convenience, a rectangular grid is used to label the molecules as shown in Fig. 1.

The potential parameters have been determined by using the nitromethane crystal as a reference case. For the intramolecular potential $W(r_{1,2})$, the potential of the predissociative state of the nitromethane molecule determined from *ab initio* calculations[13] has been fitted by Eq. (1) so that the dissociation barrier and the dissociation energy are preserved (Fig. 2). In order to obtain the intermolecular potentials, an approximate interaction potential between two nitromethane molecules has been built by the summation of Buckingham-type potentials between all atomic pairs.[15] The intermolecular potentials were then chosen so that the Morse potentials (2) give the best fits to the interactions between the NO_2 and CH_3 groups in this nitromethane interaction potential. However, a model built only on interactions between groups treated as single atoms is too simple to give a quantitative description of a real crystal like nitromethane and when the model crystal is built according to the procedure described above, the sound speed in the model is found to be too high. In order to correct this problem, we have rescaled the energies so that sound speed, measured in the numerical simulations, is in reasonable agreement with the experimental values in a molecular crystal. The final model parameters are listed in Tables I and II. They give a sound speed $v_0\approx1450$ m/s in the model crystal.

B. Numerical methods

The molecular-dynamics calculation consists in the integration of the equations of motion which result from the Hamiltonian (3). The numerical simulation of the dynamics of all the atoms in a macroscopic sample is beyond the current computation possibilities, even for a very small crystal. Therefore, the calculations have to be restricted to only one piece of the crystal, with boundary conditions selected to minimize the perturbations due to this restriction. Periodic boundary conditions with N_y cells are used in the **y** direction orthogonal to the **x** axis along which the detonation propagates. The sample can be considered as an infinite strip along **x**, but the calculation is restricted to a "computation window" containing N_x cells in the **x** direction. As the calculation evolves, the $N_x\times N_y$ window is translated in order to follow the detonation front by adding a piece of sample crystal in the front while the same number of atoms are dropped from the calculation in the back. Figure 3 shows a schematic view of the calculation window. Its translation is performed in units of $N_x/4$ cells in order to maintain at least $N_x/4$ cells of fresh sample between the shock front and the front boundary of the calculation window which is treated as a fixed boundary. The back boundary of the calculation window is free. Using such a calculation window enables us to follow the propagation of the detonation over a long distance on the molecular scale (0.25–1 μ, i.e., 500–2000 lattice cells), but we must make sure that it does not affect the numerical results. A systematic study of the role of the window size has been done in a previous work using the same approach.[16] It has shown that, at the microscopic level, the propagation of a detonation is governed by a region which extends only over a few hundred Å at most. This result is in agreement with the results obtained by Elert *et al.*[8] with a very different model including three-body interactions. This region is sufficiently small to be included in a typical calculation window of 40×10 cells or 80×20 cells. We have checked that, if the window is extended beyond this size, the structure and speed of the detonation front is not modified, except in a few specific cases which are discussed below. Thus, we can conclude that the calculation

TABLE I. Model parameters. Parameters of the intermolecular potentials.

	$V_{N\text{-}N}$	$V_{C\text{-}C}$	$V_{C\text{-}N}$
E (eV)	0.004	0.001	0.000 75
S (Å^{-1})	2.1	1.3	1.4
r_e (Å)	5.0	5.0	4.09

TABLE II. Parameters of the intramolecular predissociative potential. Mass $m_N=47$ amu, mass $m_C=15$ amu.

	V_a	V_b
E (eV)	7.934 67	8.934 67
S (Å^{-1})	1.865 0	1.574 9
r_0 (Å)	1.48	1.48

Barrier height 0.265 eV
Frequency of small intramolecular oscillations 520 cm^{-1}

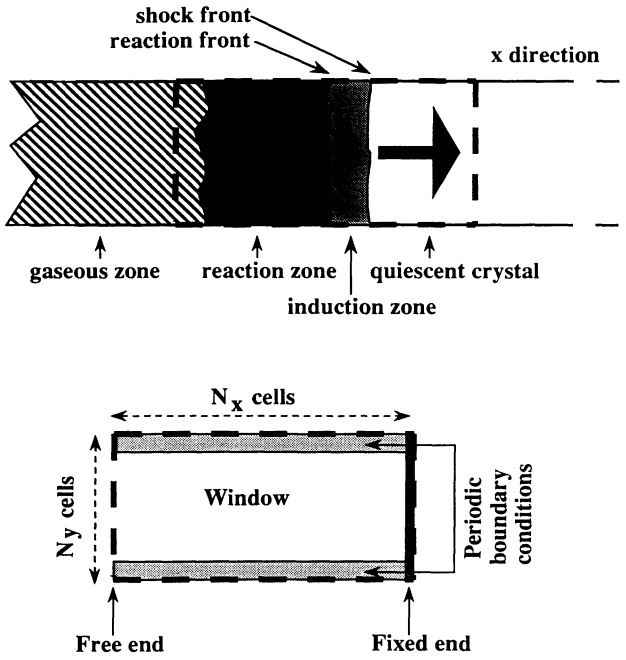

FIG. 3. Schematic view of the calculation window. The propagating shock front is kept in the third quarter of the window as the window is translated along the x direction, one quarter at a time.

window contains all the region that governs the propagation of the detonation and does not perturb our results.

The Hamiltonian equations of motion of the model crystal are integrated with a second-order Taylor algorithm,[17] and the time step is adjusted so that the changes in atomic positions never exceed 10% of the lattice unit vector during a step. This ensures that the energy in the calculation window is conserved to an accuracy of 0.05% between two translations. A typical value for the time step is 1 fs and the time unit used in the simulation is 10 fs $=10^{-14}$ s. To reduce the number of neighbors in the force calculations, a cutoff of 10 Å has been introduced in the interaction potentials. The neighbor tracking algorithm uses a mixed method of grid and atom-list bookkeeping. At the density reached in the simulations, about 48 000 atomic distances have to be calculated for each time step for a 80×20 cell calculation window which amounts to about 15 neighbors for each atom.

III. DETONATION WAVE IN A HOMOGENEOUS SAMPLE

In order to check the validity of the model and provide reference results for the investigations of the role of inhomogeneities, we have performed a first set of simulations on a homogeneous sample.

A. Characteristics of the detonation

The shock-induced detonation is initiated by applying a strong impact along the x direction on the left boundary of the sample. In the experimental studies, the initiation process can extend over several μs before a steady detonation wave is generated. In the molecular-dynamics simulations, in order to speed up the process and reach the steady state in a time scale compatible with the simulations, we apply a very strong impact which is characterized by two parameters, the time t_i during which it is applied, and the speed v_i that it would communicate during that time to a free atom, i.e., an atom not connected to its neighbors in the crystal. When a steady state is achieved, the simulation shows that the detonation wave is formed of three different regions. Starting from the front of the detonation, in the first region situated immediately behind the leading shock wave, the molecules are displaced from their equilibrium position, and a part of the shock energy is absorbed and transferred into the intramolecular bonds which are excited. We call this region the *induction zone.* The first molecular dissociations appear in a domain that we call the *reaction front* which separates the induction zone from the second region in which the intramolecular bonds are stretched over their dissociation length. In this region that we call the *reaction zone,* a large amount of potential energy is converted into kinetic energy so that the thermal motions become very large and the crystal structure begins to fall apart. Behind the reaction zone, in the third region that we call the *gaseous zone,* the energy release is over but the atoms have a very high kinetic energy and the crystal structure is completely destroyed. We call the *detonation wave* the simultaneous propagation of these three regions through the solid. The calculation window is translated with an average speed equal to the speed of the detonation wave. When a steady state is achieved, the total energy in the calculation window is constant with time over several translations, i.e., at each translation of the window, the energy lost because of the molecules dropped from the calculation (which is essentially in the form of kinetic energy) is balanced by the total energy of the fresh piece of crystal introduced in the front of the window.

Our previous results[12,10] have shown that *both* the intramolecular potential—and, in particular, the value of the energy release—and the intermolecular potentials determine whether a given crystal can sustain a detonation. For the parameters listed in Table I, the energy release is equal to 1 eV per N-C molecule (23 kcal/mol) and the crystal structure and bonding scheme meet the conditions to sustain a detonation. In particular, the crystal consists of two unequivalent sublattices. The strongly bonded N sublattice provides a rigid medium for an easy propagation of the shock, while the softer C sublattice allows for the large atomic motions that are necessary for bonds to break. The numerical simulations confirm that the model crystal can indeed sustain a steady detonation, but they exhibit *two* detonation regimes, depending on the parameters v_i and t_i of the impact.

The impact can break the first N-C molecules only if v_i exceeds a "dissociation threshold" v_s, but as long as v_i is below a second threshold v_d called the "detonation threshold," the molecular dissociations stop after a while and the detonation dies out spontaneously as in Fig. 4(a). On the contrary, when $v_i > v_d$, a steady detonation is generated but its properties depend on the duration of the

impact. For a "slow impact" during which the average acceleration of the atoms v_i/t_i is less than $a_t \approx 0.07$ Å/$(10^{-14}$ s$)^2$, the detonation propagates with a speed of about 7.5 km/s which is a characteristic of the material and not of the initial impact (in the range $v_i > v_d$ and $v_i/t_i < a_t$). We call this regime the *slow-detonation regime* [Fig. 4(b)]. A very fast impact such that $v_i/t_i > a_t$ generates a steady detonation which propagates with an extremely high speed of about 23 km/s [Fig. 4(c)]. We call this regime the *fast-detonation regime.*

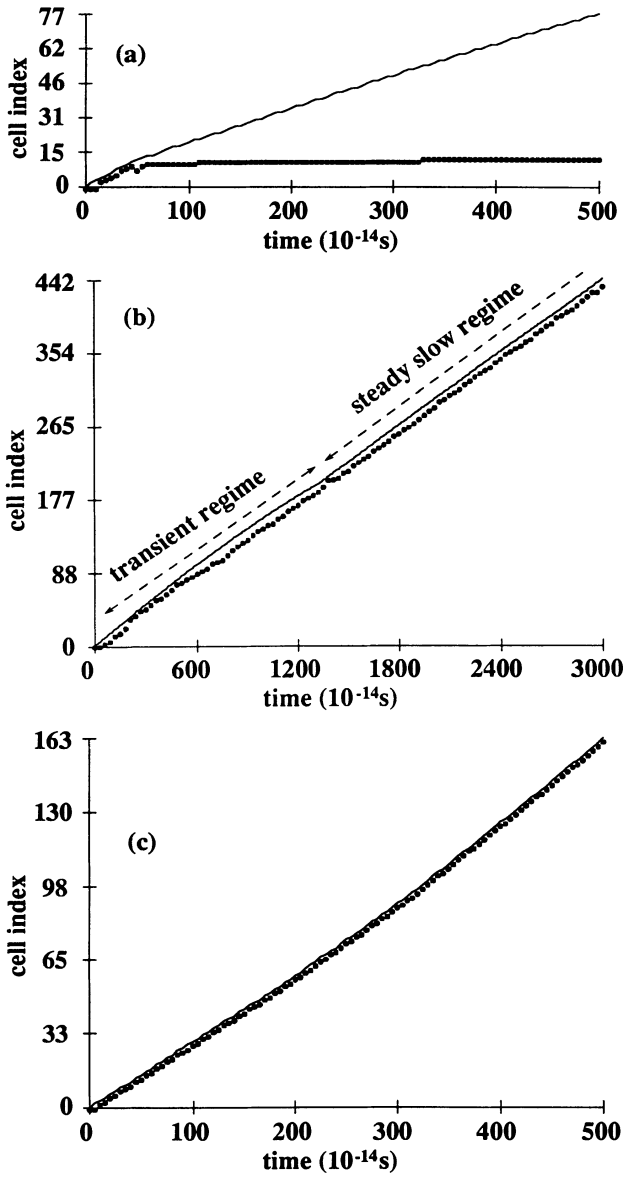

FIG. 4. Position in cells of the shock (solid line) and reaction (dots) fronts vs time for various excitation impacts: (a) Impact below the detonation threshold ($v_s < v_i < v_d$). The detonation dies out. (b) Impact above the detonation threshold but with $v_i/t_i < a_t$ (slow impact). A detonation in the slow regime is initiated. Its speed in the steady regime is 7500 m/s. (c) Fast impact above the detonation threshold ($v_i/t_i > a_t$). A steady detonation propagating at 23 200 m/s in the fast regime is initiated.

The slow- and fast-detonation regimes are qualitatively very different. In the fast regime, the induction zone is very narrow (one or two cells only) and the crystal structure is still rather well preserved in the reaction zone so that the molecular dissociations followed by the energy release occur in a coherent manner close to the shock front. Only a small part of the chemical energy is lost in disordered motions that do not sustain the detonation. This explains the extremely high detonation speed which is, however, a characteristic of the material because the same speed is obtained for all impacts in the fast range. Considering the high degree of coherence in the molecular motions required to sustain the detonation wave in the fast regime, we expect this regime to be very sensitive to perturbations. The role of defects discussed in the next section confirms this analysis.

The slow regime is more interesting because its speed is in the range of real detonation speeds. Figure 5 shows an analysis of the energy distribution in the detonation wave. The picture results from a double-averaging process, in space and in time. A sequence of snapshots of the state of the 80×20 calculation window is recorded. Each of them is divided into slices 20 Å wide and the average energy per atom is calculated in each slice to get an instantaneous energy profile. The profiles are then superimposed so that the positions of the shock front coincide in all of them, and the average energy profile is calculated. The results displayed in Fig. 5 have been averaged over 300 10^{-14} s. This averaging eliminates the effect of instantaneous fluctuations, and only the permanent features of the steady detonation wave are observed. The

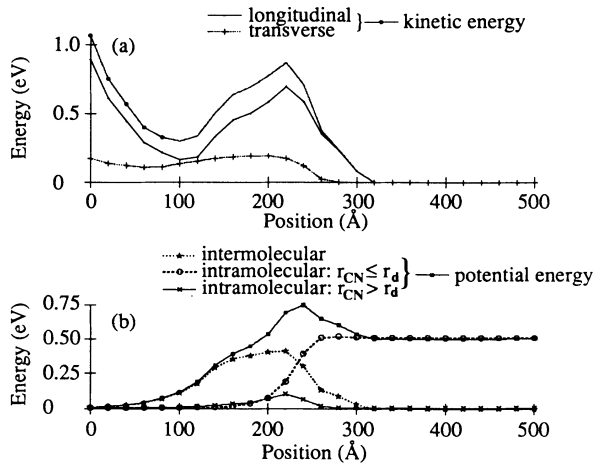

FIG. 5. Average energy profiles between $t = 2200\ 10^{-14}$ s and $t = 2500\ 10^{-14}$ s in the steady detonation regime of Fig. 4(b). (a) Kinetic energy and (b) potential energy per atom. The induction zone size is 40–50 Å. The slices used for space averaging are 20 Å wide and contain 158 atoms in the quiescent crystal. The rise of the kinetic energy per atom associated to longitudinal motions in the left part of the profile is an artefact due to the free boundary of the calculation window and should be ignored. It is due to a very small number of molecules projected back across the free boundary. The total kinetic energy carried by these few atoms is small.

first result that should be noticed in Fig. 5(a) is the large difference between the kinetic energies associated with longitudinal E_{cl} and transverse motions E_{ct} in a wide region behind the shock front. Thermal equilibration between E_{cl} and E_{ct} is only achieved 200 Å behind the leading shock. The lack of thermal equilibrium in the region where the molecular dissociations occur precludes the use of equilibrium thermodynamics and chemical kinetics to calculate reaction rates in this region. The analysis of the various components of the potential energy on Fig. 5(b) shows that the decrease in intramolecular potential energy that accompanies the dissociations starts about 40 Å behind the shock front. The induction zone is therefore much bigger in the slow-detonation regime than in the fast regime. Moreover, in the reaction zone of the slow regime, the crystal structure is so distorted that the molecules are randomly oriented. Thus, the energy release occurs in an incoherent way which is not as sufficient as in the fast regime to sustain the propagation of the shock, explaining the moderate detonation speed.

B. Role of the crystal orientation

In a polycrystalline sample, the most frequent defect is a grain boundary separating two microcrystals with different orientations. Before investigating this type of inhomogeneity, we must analyze the propagation of detonations in various directions in a homogeneous sample. We characterize the orientation of the sample by the angle α between the N-C molecule and the **x** direction in which the detonation propagates. In the reference crystal shown in Fig. 1, $\alpha=150°$. Due to the hexagonal symmetry of each N and C sub-lattices, the rotations which are compatible with the periodic boundary conditions are 60° in-plane rotations. Therefore, we have investigated the four cases, $\alpha=30°$, 90°, 150°, and 210° with impact values that generate fast and slow detonations in the reference crystal. The results are shown in Fig. 6 and they exhibit a strong difference between the two detonation regimes.

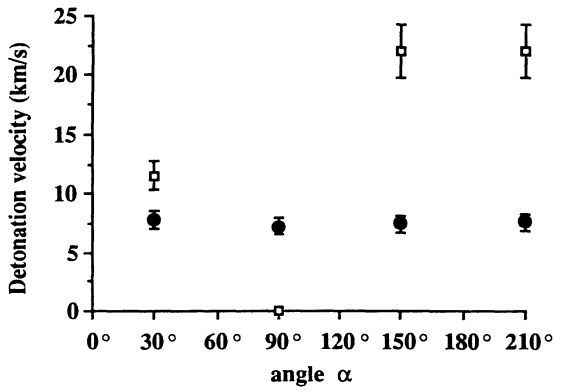

FIG. 6. Detonation velocity vs α. The squares (circles) correspond to an impact generating a fast (slow) detonation in the reference crystal. No steady detonation was observed with the fact impact for $\alpha=90°$. An estimation of the error has been done for $\alpha=150°$. The error on the detonation speed is 10%.

As expected from the coherence of the molecular motions that sustain the detonation in the fast regime, this regime is very sensitive to crystal orientation. The detonation speed of 23 km/s for $\alpha=150°$ falls down to 12 km/s for $\alpha=30°$ and in the case $\alpha=90°$, no steady detonation could be initiated by a fast impact. The extinction of the detonation in this case could result from a poor transfer of energy between the longitudinal shock wave and the intramolecular bonds which lie along the transverse direction, as it was found for the energy transfer between a pair of perpendicularly oriented molecules.[18] On the contrary, the slow regime shows a small sensitivity to crystal orientation. The detonation speed is constant within a few percent and the detonation initiated by a slow impact can propagate in the case $\alpha=90°$. The simulations show that, in this regime, whatever their initial orientation, the molecules of the induction zone rotate to reach on average a longitudinal position favorable for the transfer of energy into the intramolecular motion.

There are only few experimental studies of the effect of crystal orientation on the propagation of detonations because they require large monocrystals and are difficult to perform. In pentaerythritol tetranitrate (PETN), Dick[3] has observed a very strong effect of the crystal orientation on the ability of a sample to sustain a detonation. He has even noticed that he could not initiate a detonation along the ⟨101⟩ axis. On the contrary, in hexogene and PETN, Koch and Barras[19] found only 5% variations of the detonation speed along different crystallographic axes. It is interesting to notice that these two types of results match the two types of behavior that we find in our simulations. Although our fast regime with its extremely high detonation can certainly not represent quantitatively a real detonation, the comparison with experiments suggests that detonations in real material could differ by the degree of coherence of the molecular motions in the detonation wave. Those with a high degree of coherence would be the more sensitive to crystal structure or orientation.

IV. DETONATIONS IN AN INHOMOGENEOUS SAMPLE

The picture of the detonation wave in a solid that emerges from all the numerical simulations[5,6,8,12,15] is that of a rather narrow excitation on the molecular scale, which propagates by preserving its average shape. However, real energetic materials are not monocrystals, and even when monocrystals are used for specific experiments, they contain various types of defects. It is therefore important to determine whether the detonation wave as it appears in the numerical simulation preserves its characteristics in the presence of crystal inhomogeneities. A recent study of the propagation of shock waves in crystals with defects[20] has shown that voids can become sites of rapidly growing, thermalized, hot fluidlike phases included within the crystal lattice, but no chemistry was included in this analysis.

We have considered the most frequent type of inhomogeneities, grain boundaries (i.e. interfaces between two crystals with different orientations), small domains of a crystal with another orientation embedded in a perfect

crystal, and vacancies. In the simulations, the detonation is initiated in a piece of perfect reference crystal until a steady state is achieved. Then, instead of a simple translation of the calculation window adding a new piece of fresh crystal, we add a "defect window." Such a window consists of a piece of crystal containing the type of defect that we wish to study which has been preliminarily relaxed to a steady structure by the pseudodynamical minimization scheme used to determine the structure of the perfect crystal. When the detonation wave enters the defect window, it interacts with the defect and we analyze its behavior.

A. Grain boundaries

In this case, the defect window contains an interface which separates the reference crystal with $\alpha=150°$ from a crystal with a different orientation α' of the N-C molecules. Figure 7 shows the aspect of the relaxed interface for three values of α', $\alpha'=30°$, $\alpha'=90°$, and $\alpha'=210°$. In the first two cases, the interface is very sharp with distorsions of the crystal structure on both sides decreasing very fast from the center whereas for $\alpha'=210°$, the interface is smooth with a gradual lattice distorsion extending over several cells on both sides. In this case, $\alpha'=210°$, the crystal structure after the interface is simply derived from the crystal structure before it by switching **y** into $-$**y**. Therefore, the two structures are equivalent for a detonation propagating along **x** and the effect of the interface is restricted to the local lattice distorsion in its vicinity. The simulations show that the detonation wave, either in the fast or in the slow regime, is not perturbed by the 150°→210° interface. For the two other interfaces, the results depend strongly on the detonation regime. The slow regime is very robust and it is hardly affected by an interface [Fig. 8(a)], as one might expect from its weak sensitivity to crystal orientation. On the contrary the fast-detonation regime is severely perturbed by 150°→30° or 150°→90° interfaces. Figure 8(b) shows its behavior when it crosses the 150°→30° interface. The plane structure of the detonation is destroyed and the front breaks into narrow fingers that leave pockets of unreacted solid far behind the leading front. Simultaneously, the speed of the detonation wave falls down to 8.6 km/s, a value close to the detonation speed in the slow regime, but the structure of the front with its fingers is still very different from that of a detonation wave in the slow regime. Since the studies of the role of the crystal orientation have shown that a detonation in the fast re-

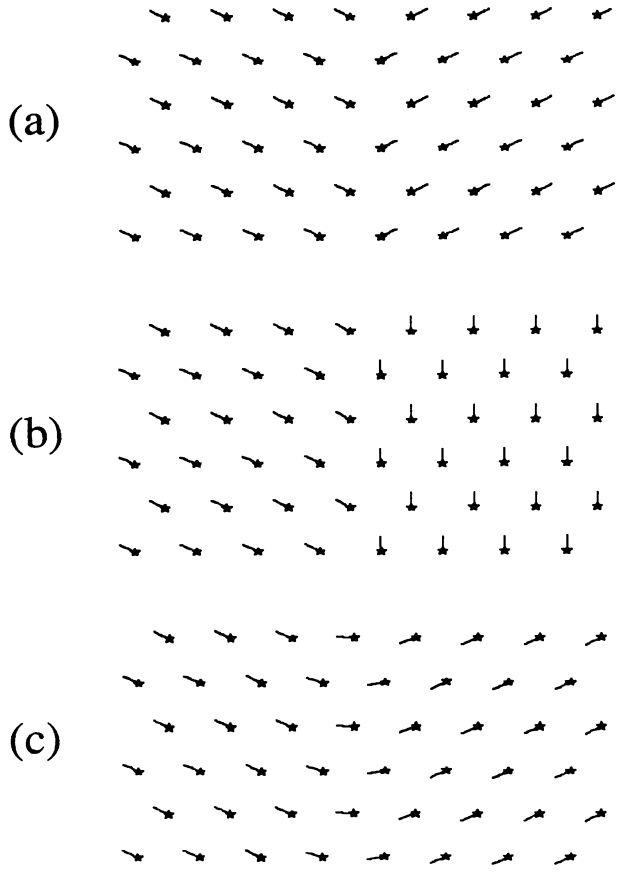

FIG. 7. Examples of defect windows for grain boundaries after minimizations. (a) 150°→30° interface. (b) 150°→90° interface. (c) 150°→210° interface.

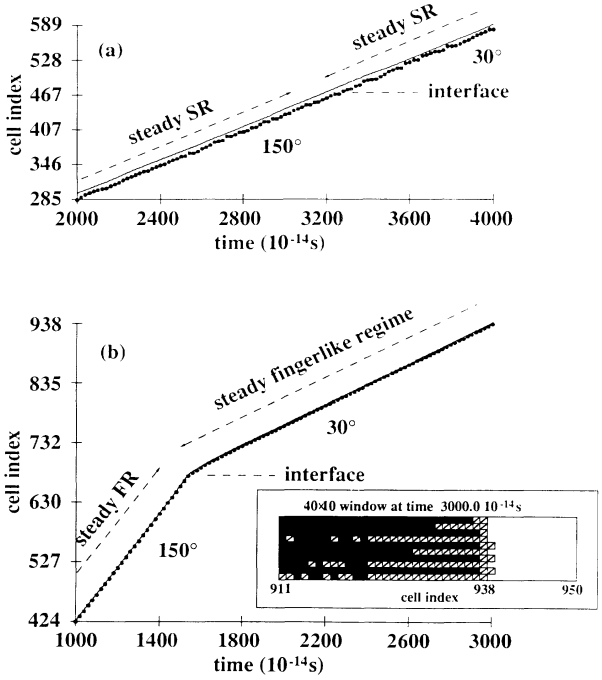

FIG. 8. Propagation of a detonation initiated in the reference crystal through the 150°→30° interface. (a) Detonation propagating initially in the slow regime. The interface causes only transient fluctuations of the induction zone size. (b) Detonation propagating initially in the fast regime. Inset: view of the 40×10 calculation window after the detonation has crossed the interface. The black cells contain dissociated molecules, the shaded cells contain molecules excited by the shock but not broken (induction zone), and the white cells are the cells not yet reached by the shock. The detonation slows down to 8.6 km/s and, as shown in the inset, the planar front evolves into a structure containing several fingers.

gime could not be initiated in a lattice with $\alpha=90°$, one could expect that the $150°\rightarrow 90°$ interface would kill completely the detonation wave. This is not the case. As in the $150°\rightarrow 30°$ case, the planar front is unstable, but instead of breaking into several fingers, only one finger is generated within the width of one calculation window. Its extremity accelerates up to 43 km/s while the detonation does not extend into the transverse direction. We have not been able to check the stability of this narrow front for a long time because its extremely high speed requires translation of the calculation window too often and the reaction zone is finally completely dropped from the calculation. This is one example where the window perturbs the results. The instability of the planar detonation front in the fast regime is reminiscent of the instability of the interface in fluid solidification when a sample is pulled at a given speed in an imposed temperature gradient around its melting temperature.[21] Below a critical speed, the solidification front is planar while above the planar interface is unstable and presents dendrites. This analogy is interesting from a fundamental point of view and would deserve further investigations. However, we have not investigated this point further here because the fast regime in our model, with its extremely high speed, is unlikely to correspond to a type of detonation wave observable in real systems.

B. Domains

The defect that we consider now consists of a strip of a crystal rotated with respect to the reference crystal, embedded in the reference crystal. In this case, the defect window consists of two successive interfaces $\alpha=150°\rightarrow\alpha'$ and $\alpha'\rightarrow\alpha=150°$, separated by d cells. Such a defect is henceforth denoted as a $d-\alpha'$ domain. Figure 9 shows several examples of such defects with $d=12$. Since the defects are localized in a few rows, one could expect that such domains would cause only a temporary perturbation of the steady detonation which would then recover its original structure and speed. This is true for most of the cases investigated like the 12-90° or 12-210° domains, for both the fast and slow regimes, but not for the 12-30° which kills the detonation wave in the two regimes. As shown in Fig. 9(a), the second interface in this case is associated to rather large crystal distortions and includes a region in which the molecules are transversally oriented. Thus, it subjects the detonation wave to a strong perturbation which comes soon after the perturbation caused by the first interface. This may explain why the cumulative effect of the two interfaces in the 12-30° domain is so drastic. A few N-C molecules are dissociated after the second interface, but the detonation cannot recover a steady state and eventually dies out.

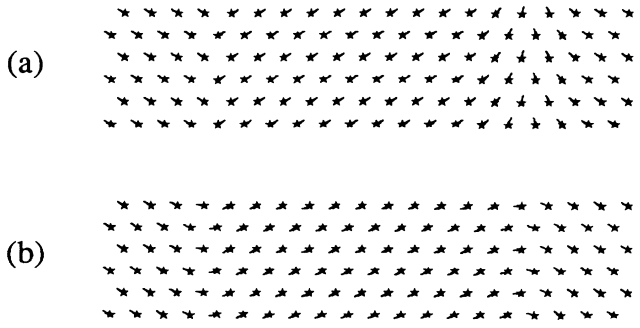

FIG. 9. Examples of defect windows with domains. (a) 12-30° domain in which 12 rows of crystal with $\alpha'=30°$ were embedded in a piece of reference crystal and relaxed to a steady state. (b) 12-210° defect window.

C. Vacancies

In our calculations, vacancies extending over 12 cells along **x** are obtained by filling them with dummy molecules which have no interactions with the others. As the other defect windows, they are relaxed to an equilibrium configuration prior to their introduction in front of the steady detonation. In a recent work Tsai[23] has shown that, under the rapid compression of a crystal, the structural relaxation around vacancies can cause a considerable local heating. The first studies of the role of vacancies on a detonation wave were performed by Hardy, Karo, and Walker.[22] They found that a row of atoms was projected into the vacancy and initiated a new detonation on the opposite side. This is also what we find in our calculations for a detonation propagating in the fast regime [Fig. 10(a)]. Due to the high degree of coherence

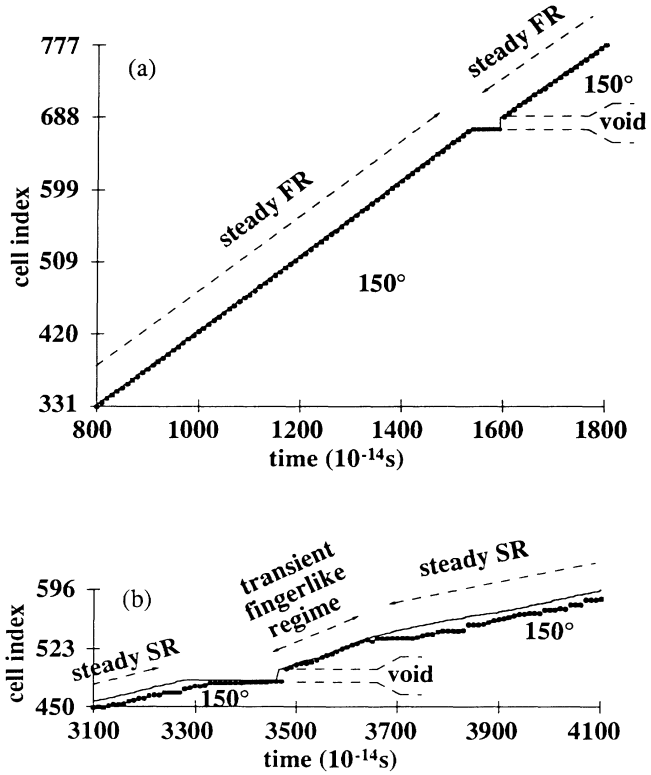

FIG. 10. Propagation of a detonation initiated in the reference crystal across a 12-column-wide vacancy. (a) A detonation in the fast regime (FR) restarts instantaneously after crossing the void. (b) A detonation in the slow regime (SR) develops a transient faster fingerlike structure after the void and then recovers its steady state.

of the atomic motions in this regime, the N atoms of the last column of N-C molecules are projected together across the void where they travel almost freely at high speed before colliding on the opposite side with the atoms of the quiescent crystal. Their impulse is sufficient to initiate a detonation on the opposite side of the vacancy so that the detonation in the fast regime crosses the vacancy with only a small perturbation. A detonation in the slow regime can also cross the vacancy, but, since the atomic motions are disordered in this regime, the excitation of the quiescent crystal by the atoms having crossed the vacancy is inhomogeneous. This generates a detonation front with fingers similar to the one mentioned previously for the fast regime across an interface. In this stage, the detonation accelerates but a fingerlike front is not stable in the slow regime. After some transient state, the slow regime detonation recovers its steady structure with a planar front and initial speed [Fig. 10(b)]. Therefore, although the collapse of the vacancy causes a temporary speed up of the detonation, this effect is very limited in time, at least with the size of the vacancies that we have investigated (12 cells).

D. Hot spots

Finally, since hot spots are often invoked as a possible mechanism sustaining the propagation of a detonation, we have considered the particular case of a detonation wave coming toward a site in which a reaction started locally slightly earlier. This is achieved by placing ahead of the leading shock a highly reactive site, obtained by approaching together to a distance smaller than their equilibrium distance the N and C atoms of a molecule. The two atoms repel strongly and the molecule dissociates violently, initiating other reactions in its neighborhood.

As for the other types of defects, the slow detonation is much more robust than the fast one when it encounters an already reacted region, as shown in Fig. 11(a). The distance between the leading shock and the reaction front increases significantly when the detonation reaches the region in which the population of unreacted molecules has been depleted, but the reaction eventually catches up and the steady regime is recovered. The behavior of a detonation moving in the fast regime arriving on the "hot spot" is displayed in Fig. 11(b), which shows that the size

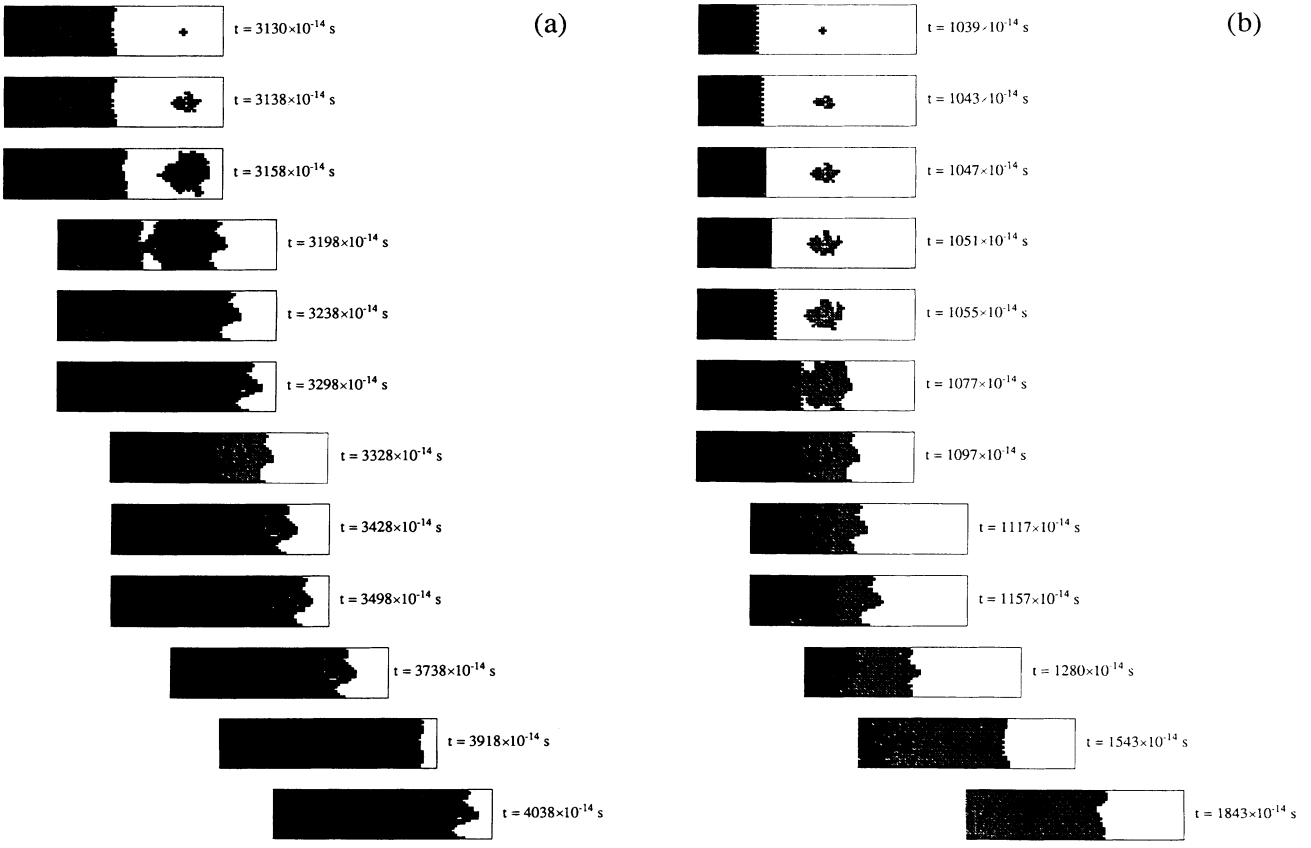

FIG. 11. Snapshots of a detonation interacting with a "hot spot," i.e., a small region where the reaction started locally before it is reached by the detonation wave. The white cells represent the quiescent material, the shaded cells have been excited by the shock but the molecules are not dissociated, the black cells contain dissociated molecules. The horizontal translations of the figures correspond to the translation of the calculation window. (a) Detonation in the slow regime. The size of the induction zone increases temporarily, but the detonation is able to recover its steady state. (b) Detonation in the fast regime. The hot spot exhausts the population of unreacted molecules and the detonation dies out.

of the induction zone increases when the detonation moves across the region of already reacted molecules, and finally the detonation dies out, leaving only a shock wave unable to cause new dissociations. This result may seem in contradiction with the common idea that hot spots favor the propagation of a detonation. However, in the case investigated here, the hot spot was so hot that local reactions could start before the arrival of the detonation front. The net effect then was to exhaust the population of unreacted molecules able to release energy to sustain the propagation of the front. Such a particular hot spot is nothing other than a "counterfire" able to kill a detonation in the fast regime because it destroys its organized structure.

V. DISCUSSION AND CONCLUSION

Except for systems as simple as the argon gas, the validity of results obtained from numerical simulations of a model are subjected to the validity of the model from which they are derived, and must therefore be taken with caution. The simulations presented in this paper have exhibited *two* regimes for the propagation of a detonation in a model crystal. The slow regime, which has a detonation speed in agreement with the speeds found in experiments on energetic materials, can be expected to provide a "realistic" microscopic description of a detonation wave. On the contrary, the fast-detonation regime with its extremely high speed is unlikely to correspond to any real detonation. Moreover, preliminary simulations with a nonzero-temperature sample indicate that the fast regime does not persist at moderate temperature. Therefore, the temptation is high to conclude that this regime is an unphysical peculiarity of the model that should be ignored. However, the previous numerical simulations of detonations at the microscopic level, performed with very different models[22,6,12,8] (one-, two-, or three-dimensional models using predissociative potentials, phenomenological models, or three-body potentials to represent the chemistry) have exhibited many common features of the detonation wave. For instance, all the calculations agree on the small width of the shock front or moderate size of the induction zone at the molecular scale. This shows that the results are only weakly sensitive to the details of the model, provided it is built on reasonable physical assumptions. This is fortunate since, otherwise, any attempt to investigate the microscopic structure of a detonation wave from the numerical treatment of a model would be in vain because the model is always oversimplified with respect to the complex physical and chemical phenomena involved in a detonation. This conclusion may mean that, in spite of its peculiarities, the fast-detonation regime found in a particular model may not be so unphysical. Perhaps the main idea that emerges when one examines its properties is that, in some specific systems properly excited, there could exist detonations which propagate with a high degree of coherence of the molecular motions in the vicinity of the shock front. Even if the coherence of the motions in a real energetic material is not as high as in our model system excited by a fast impact, the high sensitivity of this type of detonation to crystal orientation or defects should subsist. Therefore, a detonation similar to our fast-detonation regime can only be expected in high-quality samples. The instability of the planar front in the fast regime and its tendency to form fingers reminiscent of the instability of solidification fronts is an interesting fundamental question that would deserve further investigations because it could provide some information to help designing a model for a detonation wave in a crystal.

The slow-detonation regime, which is likely to represent the detonation regime in most of the real materials, is much more robust. The numerical simulations presented here have shown its weak sensitivity to crystal orientation and to most of the defects. We have observed that the collapse of vacancies, a mechanism often assumed as important to create "hot spots" that favor the propagation of the detonation, can accelerate temporarily the detonation. However, with the size of the vacancies considered in this study, this effect is limited. Therefore, the slow-detonation regime could survive in a polycrystalline sample similar to the powders used in experiments. This shows that the microscopic picture of a detonation wave that emerges from the molecular-dynamics studies is compatible with a real sample. This microscopic picture contains an important feature for modeling detonations in solids. Although the size of the induction zone is much larger in the slow regime than in the fast one, the simulations show that thermal equilibrium is not achieved in the induction zone. This lack of equilibrium should be included in the analysis of the chemical reaction kinetics for solid-state detonations.

ACKNOWLEDGMENTS

The authors would like to thank E. Oran for a critical reading of a first version of this manuscript. A large part of this work has been sponsored by a contract between Direction des Recherches, Etudes et Techniques (DRET France) and the Départment de Recherches Physiques, groupe Chimie Quantique (Université P. et M. Curie, Paris). We also acknowledge a grant of computer time on the IBM 3090-400E-3VF computer at the Centre National Universitaire Sud de Calcul (Montpellier, France) under a collaboration on the theme "High Performance Computing" developed by the Centre de Compétence en Calcul Numérique Intensif.

[1]Approches Microscopique et Macroscopique des Détonations (Megève, France), edited by S. Odiot, les Editious de Physique [J. Phys. (Paris) Colloq. C4, **48**, (1987)].

[2]P. Rudel, S. Odiot, J. C. Mutin, and M. Peyrard, J. Chim. Phys. **87**, 1307 (1990).

[3]J. J. Dick, Appl. Phys. Lett. **44**, 859 (1984).

[4]H. N. Presles, M. Hallouin, and P. Harris, J. Phys. (Paris) Colloq. **48**, C4-127 (1987).

[5]A. M. Karo, J. R. Hardy, and F. E. Walker, Acta Astronaut. **5**, 1041 (1978).

[6]D. H. Tsai and S. F. Trevino, J. Chem. Phys. **81**, 5636 (1984).
[7]S. F. Trevino and D. H. Tsai, in *Proceedings of the Eighth Symposium (International) on Detonation, Albuquerque,* edited by J. M. Short (Naval Surface Weapon Center, White Oak, Silver Spring, Maryland, 1986), p. 870.
[8]M. L. Elert, D. M. Deaven, D. W. Brenner, and C. T. White, Phys. Rev. B **39**, 1453 (1989).
[9]D. H. Tsai (private communication).
[10]S. G. Lambrakos and M. Peyrard, J. Chem. Phys. **93**, 4329 (1990).
[11]M. Peyrard, S. Odiot, and M. Blain, J. Chim. Phys. (Paris) **85**, 759 (1988).
[12]M. Peyrard, S. Odiot, E. Oran, J. Boris, and J. Schnur, Phys. Rev. B **33**, 2350 (1986).
[13]C. Mijoule, S. Odiot, S. Flizar, and J. M. Schnur, *THEOCHEM* (Elsevier Scientific, Netherlands, 1987), Vol. 149, p. 311.
[14]R. Hockney and J. W. Eastwood, *Computer Simulations Using Particles* (Hilger, London, 1988).
[15]M. Peyrard, S. Odiot, E. Lavenir, and J. M. Schnur, J. Appl. Phys. **57**, 2626 (1985).
[16]S. G. Lambrakos, M. Peyrard, E. S. Oran, and J. P. Boris, Phys. Rev. B **39**, 993 (1989).
[17]R. W. Stanley, Am. J. Phys. **52**, 499 (1984).
[18]Chen Zhiying, Ding Jiaquiang, and D. H. Tsai, Acta Mech. Sin. **4**, 372 (1988).
[19]H. W. Koch and J. C. Barras (unpublished).
[20]L. Phillips, E. S. Oran, and J. P. Boris (unpublished).
[21]P. Kurowski, C. Guthmann, and S. de Cheveigné, Phys. Rev. A **42**, 7368 (1990).
[22]J. R. Hardy, A. M. Karo, and F. E. Walker, Prog. Astronaut. Aeronaut. **75**, 209 (1981).
[23]D. H. Tsai (unpublished).

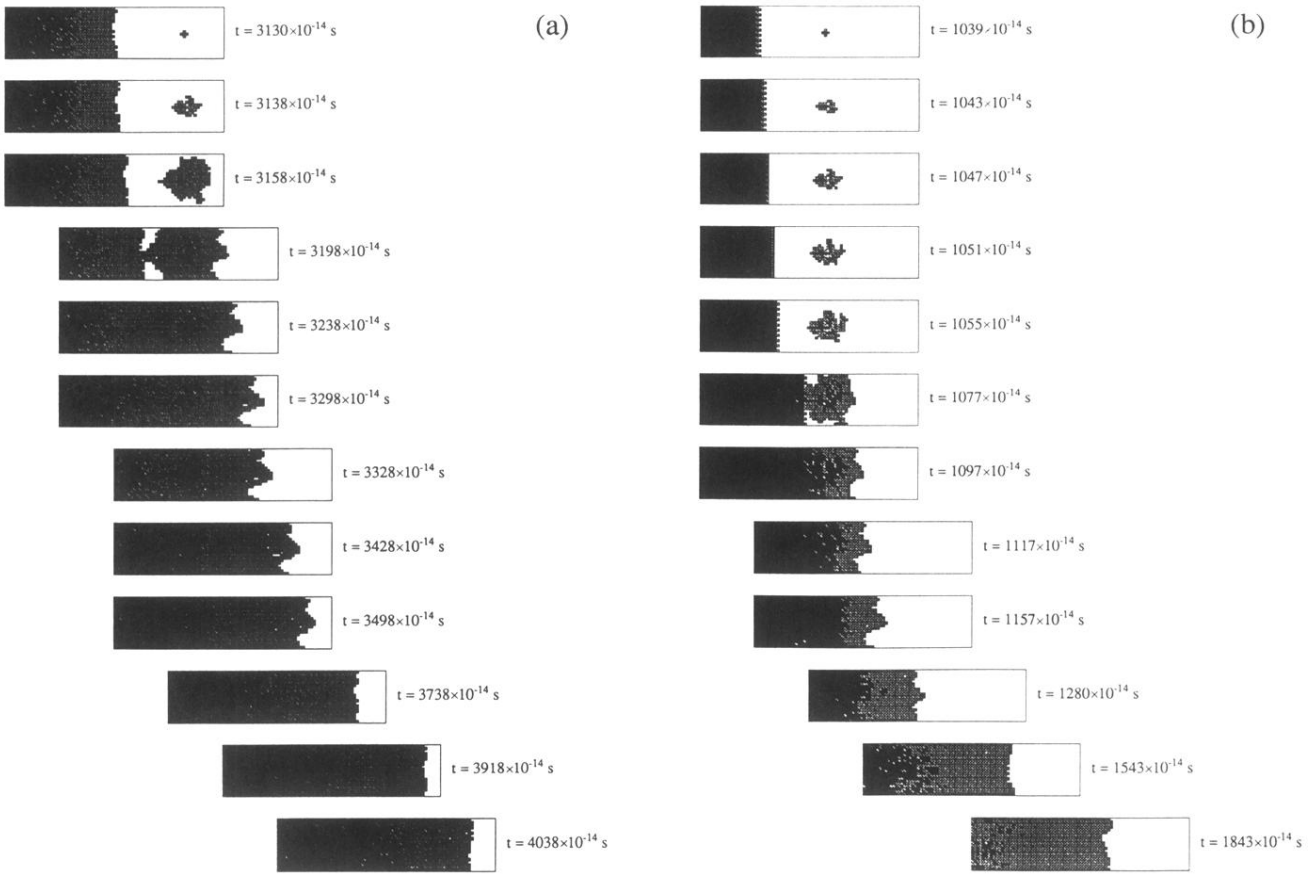

FIG. 11. Snapshots of a detonation interacting with a "hot spot," i.e., a small region where the reaction started locally before it is reached by the detonation wave. The white cells represent the quiescent material, the shaded cells have been excited by the shock but the molecules are not dissociated, the black cells contain dissociated molecules. The horizontal translations of the figures correspond to the translation of the calculation window. (a) Detonation in the slow regime. The size of the induction zone increases temporarily, but the detonation is able to recover its steady state. (b) Detonation in the fast regime. The hot spot exhausts the population of unreacted molecules and the detonation dies out.

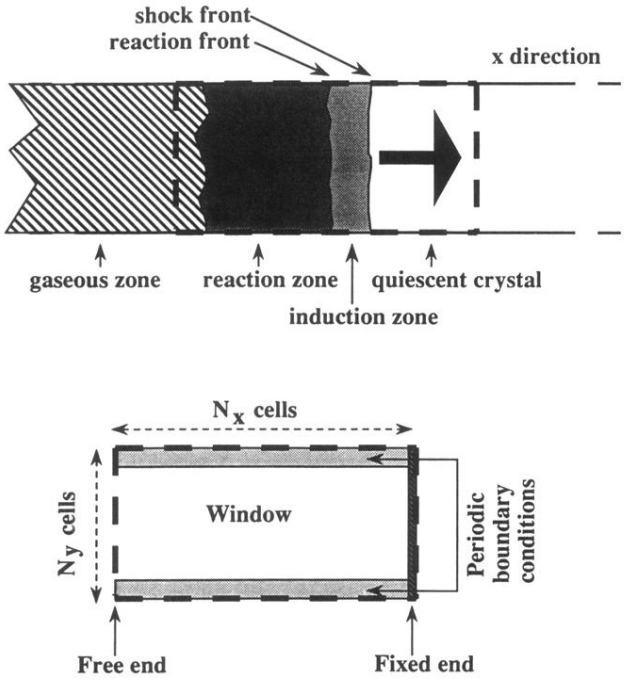

FIG. 3. Schematic view of the calculation window. The propagating shock front is kept in the third quarter of the window as the window is translated along the **x** direction, one quarter at a time.